Inversion asymmetry spin splitting in self-assembled quantum rings

Fabrízio M. Alves,[1] C. Trallero-Giner,[2] V. Lopez-Richard,[1] and G. E. Marques[1]
[1]*Departamento de Física, Universidade Federal de São Carlos, 13560-905, São Carlos, São Paulo, Brazil*
[2]*Department of Theoretical Physics, Havana University, Vedado, 10400 Havana, Cuba*
(Received 30 October 2007; revised manuscript received 2 January 2008; published 28 January 2008)

We report theoretical studies of the spin splitting caused by inversion asymmetries in quantum ring-shaped self-assembled quantum dots with circular cross sections. We analyze the conduction band and the spin-splitting electronic energy dispersions of the system in the presence of both bulk (Dresselhaus) and structural (Rashba) inversion asymmetries as a function of quantum ring geometrical parameters. We have explored the interplay effects between the circular confinement symmetry and the magnitude of the spin-orbit constants for the dot material. We describe universal conditions to operate a spin-field-effect transistor based on quantum rings with identical linear Dresselhaus and Rashba spin-orbit coupling interactions. The results show to be sensitive to both the quantum ring radii and the dot thickness.

DOI: 10.1103/PhysRevB.77.035434 PACS number(s): 73.21.La, 71.70.Ej, 73.22.Dj

I. INTRODUCTION

The search for controlling conditions on the manipulation of spin-orbit (SO) interaction in semiconductor nanostructures is one highly appealing subject for spintronic devices, quantum information, and quantum computing.[1–4] The understanding of how SO couplings occur and how to manipulate the spin degree of freedom, combined with the application of external fields, are important challenges for the realization of these devices.[5,6] Asymmetries in the spatial confinement (Rashba effect)[7] and the intrinsic bulk form that exists in zinc-blende crystals (Dresselhaus interaction)[8] strongly affect the spin-polarized optical and transport as well as the spin relaxation properties of carrier states in nanostructures.

Spin-field-effect transistor (SFET) for electrons moving in quasi-one-dimensional wires was proposed in the past.[9] Moreover, the Rashba term can be tuned by applying a gate voltage or by doping, which allows the competition between these two forms of SO interactions and leading, in principle, to long spin lifetime for the injection of electron-spin-polarized currents. Based on this fact and on the optimization of the spin-diffusion length in GaAs quantum well, a nonballistic SFET was proposed in Ref. 4. The annihilation of the spin splitting induced by the SO interaction will affect the conductance in persistent currents through the ring. The effects of the SO interaction on spin-polarized currents in quantum rings have been profusely discussed (see Refs. 10 and 11). The main effect attributed to the SO interaction, in these cases, is the removal of some degeneracy related to spin orientation. However, few discussions have been devoted to the combined effect of SO interactions of different nature and the possibility of the mutual annihilation of their influence. This would lead to the modulation of the spin interference that creates oscillations in the conductance of spin resolved currents. An important and fundamental problem for the ability of any particular geometry to be successful in future applications concerns the studies of transport properties when two or more leads are attached to the system. Similar studies have been carried out in Refs. 10 and 12 on the conductance properties of a two-dimensional quantum circular billiard with two leads. In the framework of the Landauer formula, it was concluded that the shape and the relative position of leads affect the transport properties of the billiard.[10]

Nowadays, using molecular beam epitaxy is possible to grow self-assembled ringlike semiconductor structures in a large range of inner and outer radii. Typical samples show a circular cross section with an inner radius about 10 nm, and the outer radius ranges between 30 and 70 nm.[13–17] This kind of structures has been studied by their potential applications as spintronic and quantum computing.[15,16,18,19] For example, it has been argued that the electron spin in quantum rings (QRs) with SO interaction is a good candidate for quantum information processing.[20]

Under these motivations, we will describe in this paper the effects induced by the QR spatial geometry and by the SO interactions on the electronic states of the zinc-blende-type semiconductor nanostructures. The total single-particle Hamiltonian for a QR with circular cross section of inner (outer) radius r_1 (r_2) and height L_z in the presence of bulk inversion asymmetry (BIA) has the form[8]

$$\mathcal{H} = \mathcal{H}_0 + \delta\sigma \cdot \kappa, \tag{1}$$

$$\mathcal{H}_0 = \frac{\hat{\mathbf{p}}^2}{2m^*} + V(\mathbf{r}, z), \tag{2}$$

where m^* is the electron effective mass, $V(\mathbf{r},z)$ is the spatial confinement for $\mathbf{r}=(x,y)$ and z along the ring axis, δ is the Dresselhaus SO constant for the material, $\sigma=(\sigma_x,\sigma_y,\sigma_z)$ is the vector of Pauli spin matrices, and κ is vector operator with components $\kappa_x=\hat{k}_y\hat{k}_x\hat{k}_y-\hat{k}_z\hat{k}_x\hat{k}_z$ (cyclic permutations for κ_y and κ_z).

If we assume a narrow QR with the z direction grown along [001], the Dresselhaus SO term in Eq. (1) is reduced to the in-plane Hamiltonian

$$\mathcal{H}_{SO} = \delta\{\sigma_x\hat{k}_x(\hat{k}_y^2 - \langle\hat{k}_z^2\rangle) + \sigma_y\hat{k}_y(\langle\hat{k}_z^2\rangle - \hat{k}_x^2) + \sigma_z\langle\hat{k}_z\rangle(\hat{k}_x^2 - \hat{k}_y^2)\}, \tag{3}$$

where the mean values $\langle\hat{k}_z^2\rangle$ and $\langle\hat{k}_z\rangle$ are taken over the ground state along the z direction. Due to parity symmetry,

$\langle \hat{k}_z \rangle \approx 0$. Thus, the effective SO Hamiltonian for a ring assumes the form $\mathcal{H}_{SO}=\mathcal{H}_{1D}+\mathcal{H}_{3D}$, where

$$\mathcal{H}_{1D} = -\delta \langle \hat{k}_z^2 \rangle (\hat{k}_+ \sigma_+ + \hat{k}_- \sigma_-) \tag{4}$$

represents the k-linear BIA contribution while

$$\mathcal{H}_{3D} = \frac{\delta}{4}(\hat{k}_+^2 - \hat{k}_-^2)(\hat{k}_- \sigma_+ + \hat{k}_+ \sigma_-) \tag{5}$$

correspond to the k-cubic BIA correction that is generally considered a perturbation term. In Eqs. (4) and (5), $\sigma_\pm = \frac{1}{2}(\sigma_x \pm i\sigma_y)$ and $\hat{k}_\pm = (\hat{k}_x \pm i\hat{k}_y)$.

II. INVERSION ASYMMETRY SPIN SPLITTING

In the derivation of the Hamiltonian (3), it is assumed the adiabatic approximation which allows us to decouple the xy plane from the z axis motions. This approach is well justified for QRs under the flat condition $r_2 - r_1 \gg L_z$ that is fulfilled for typical self-assembled ringlike structures.[15,16] Thus, the adiabatic single-particle wave, in the absence of SO, is factored as[21,22]

$$\Psi_{n,m,\nu}(\mathbf{r},z) = \psi_{n,m}(\mathbf{r})\Phi_\nu(z), \tag{6}$$

where $\Phi_\nu(z)$ represents the νth vertical confined state along the z axis with energy $E_\nu^{(0)}$ and $\psi_{n,m}(\mathbf{r})$ gives the lateral or radial confined states. Since the QR structures have width around 300 Å,[14] we may assume an infinite barrier at the cylindrical surface and $V(\mathbf{r},z)=0$ for $\mathbf{r} \in \mathbf{r}_2 - \mathbf{r}_1$. Therefore, the xy-motion wave function $\psi_{n,m}(\mathbf{r})$, solution of Hamiltonian (2), can be written in the form (see Ref. 21)

$$\psi_{n,m}(r,\theta) = \frac{1}{\sqrt{2\pi}} R_{n,m}(r) e^{im\theta},$$

$$R_{n,m}(r) = A_{n,m}\left[N_{|m|}(\mu_n^{(m)}) J_{|m|}\left(\mu_n^{(m)} \frac{r}{r_1}\right) - J_{|m|}(\mu_n^{(m)}) N_{|m|} \times \left(\mu_n^{(m)} \frac{r}{r_1}\right)\right],$$

$$= A_{n,m} \mathcal{Z}_m\left(\mu_n^{(m)} \frac{r}{r_1}\right), \tag{7}$$

where $J_m(x)$ $[N_m(x)]$ is the Bessel (Neumann) function of mth order, $m=0, \pm 1, \pm 2, \ldots$, is the z component of the orbital angular momentum, and $n=1,2,3,\ldots$, is the radial quantum number. Also, $A_{n,m}$ is the normalization constant given by[23]

$$A_{n,m} = \frac{1}{r_1} \sqrt{\frac{2}{\left(\frac{r_2}{r_1}\right)^2 C_m\left(\mu_n^{(m)}, \frac{r_2}{r_1}\right)^2 - C_m(\mu_n^{(m)}, 1)^2}}, \tag{8}$$

with

$$C_m(a,b) = N_{|m|}(a) J_{|m|-1}(ab) - J_{|m|}(a) N_{|m|-1}(ab). \tag{9}$$

The corresponding lateral eigenenergies are $E_{n,m}=(\mu_n^{(m)})^2 E_0$, where $E_0=\hbar^2/(2m^* r_1^2)$ and $\mu_n^{(m)}$ is the nth root of the mth order transcendental equation

$$\frac{N_{|m|}(\mu_n^{(m)})}{N_{|m|}\left(\mu_n^{(m)} \frac{r_2}{r_1}\right)} = \frac{J_{|m|}(\mu_n^{(m)})}{J_{|m|}\left(\mu_n^{(m)} \frac{r_2}{r_1}\right)}. \tag{10}$$

Assuming that the k-cubic term (5) gives a small correction to the eigenenergy values, it will not be included in the calculations but few effects will be discussed later. The k-linear SO contribution for the cylindrical QR can be written as

$$\mathcal{H}_{1D} = -i\gamma \begin{bmatrix} 0 & \exp(-i\theta) p_{r,\theta}^- \\ \exp(+i\theta) p_{r,\theta}^+ & 0 \end{bmatrix}, \tag{11}$$

where $\gamma = -(\pi/d)^2 \delta$ and $p_{r,\theta}^\pm = \left[\frac{\partial}{\partial r} \pm \frac{i}{r}\frac{\partial}{\partial \theta}\right]$. This term has to be added to Eq. (2) yielding the full Hamiltonian $\mathcal{H}=\mathcal{H}_0+\mathcal{H}_{1D}$, which does not allow an explicit close solution for the wave function. The SO interaction breaks the axial symmetry and (n,m) are not good quantum numbers anymore. It is possible to show that the set of wave functions (7) is a complete set for the description of the electronic motion on the xy plane. According to the structure of the $\mathcal{H}_{1D}$ the general solution of $\mathcal{H}$ can be searched as

$$\Psi(\mathbf{r}) = \sum_{n'} \begin{bmatrix} a_{n',m}^{(1)} \psi_{n',m} |\uparrow\rangle \\ a_{n',m+1}^{(2)} \psi_{n',m+1} |\downarrow\rangle \end{bmatrix}, \tag{12}$$

where $a_{n,m}^{(1)}$ and $a_{n,m}^{(2)}$ are weight coefficients of the linear combination for the spin-up ($|\uparrow\rangle$) and spin-down ($|\downarrow\rangle$) components of the spinor state. They depend on the aspect ratio and on the BIA parameter γ. Using Eq. (12), the solutions for the Hamiltonian $\mathcal{H}=\mathcal{H}_0+\mathcal{H}_{1D}$ can be obtained from the set of dimensionless coupled equations:

$$\sum_{n'} \begin{pmatrix} (\mu_n^{(m)})^2 \delta_{n',n} & i\gamma_D f^- \\ -i\gamma_D f^+ & (\mu_n^{(m+1)})^2 \delta_{n',n} \end{pmatrix} \begin{pmatrix} a_{n',m}^{(1)} \\ a_{n',m+1}^{(2)} \end{pmatrix} = \lambda \begin{pmatrix} a_{n',m}^{(1)} \\ a_{n',m+1}^{(2)} \end{pmatrix}. \tag{13}$$

Here, $\lambda = E/E_0$ labels the new electronic states, $\gamma_D = -\gamma/(r_1 E_0)$, and $f^\pm$ are the dimensionless matrix elements defined in the Appendix.

Observe, in Eq. (13), that the mixing induced by the bulk inversion asymmetry brakes the spin degeneracy of states. The interaction $\mathcal{H}_{1D}$ couples different spin orientated components with $\Delta m = \pm 1$. As a consequence, the spinors $\Psi(\mathbf{r})$ are restricted to two independent Hilbert subspaces, labeled I and II, that are classified according to the parity of the orbital quantum number m and spin orientation. In subspace I, we are grouping spinor states with spin-up components having m even and spin-down components having m odd. In the orthogonal subspace II, the spinor states have spin-down components with m even and spin-up components having m odd. Hence, the set of equations (13) for a given m can be

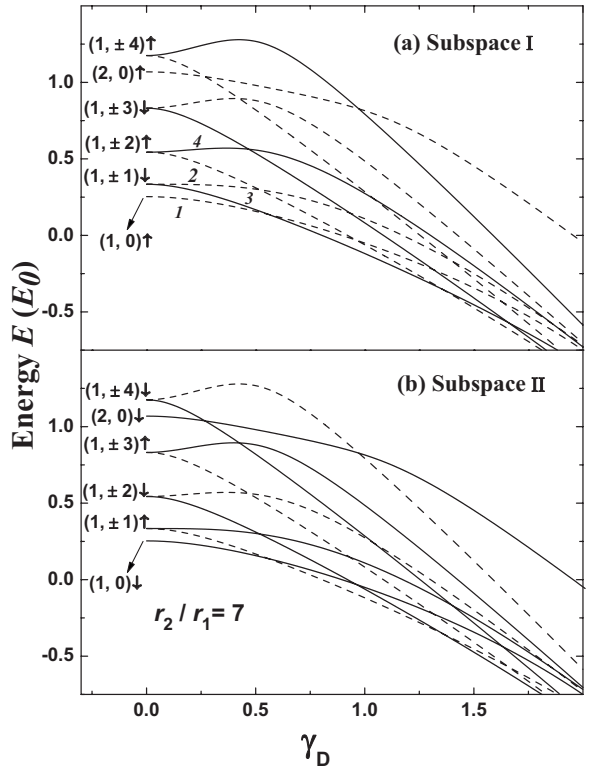

FIG. 1. The first ten eigenenergies E in units of E_0, solution of Eq. (13), as a function of the dimensionless spin-orbit Dresselhaus parameter $\gamma_D=-\gamma/(r_1E_0)$. The energies are labeled as $(n,\pm m)$ and spin orientation according to the zero-SO character of the quantum ring. Panel (a) represents those independent solutions with even (odd) quantum number m and spin up (down). (b) corresponds to m odd (even) numbers and spin down (up). Solid and dashed lines show those states which are couple for a particular $(m\pm 1)$ z component of the quantum angular momentum m (see text).

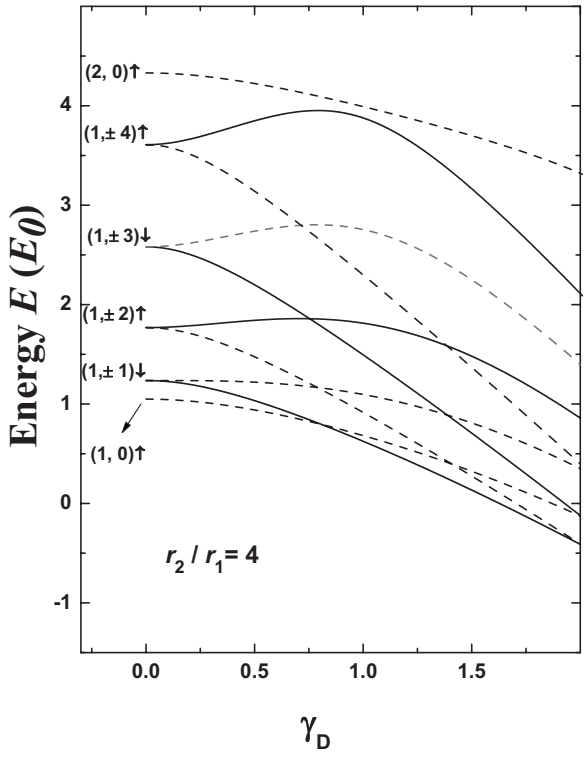

FIG. 2. The same as in Fig. 1 for the quantum ring aspect ratio $r_2/r_1=4$.

solved independently for each Hilbert subspace I and II.

In Fig. 1, we want to show the effects caused by the linear BIA term on the first ten quantum ring energy levels in each Hilbert subspace as a function of the normalized SO parameter γ_D. The levels were labeled according to the zero-SO character as $(n,\pm m)$ and spin state orientation $|\uparrow\rangle$ or $|\downarrow\rangle$ of the $\mathcal{H}_0$ states. Due to symmetry of the QR and in the absence of the SO interaction for a given eigenenergy $E_{n,m}$, there are four degenerate states, namely, $|n,\pm|m|;\uparrow\rangle$ and $|n,\pm|m|;\downarrow\rangle$. The solutions for subspaces I and II are shown in panels (a) and (b) of Fig. 1, respectively. It can be seen that the energy eigenvalues decrease as γ_D increases. Furthermore, solid and dashed lines in these panels represent those states which are coupled for a particular m value according to the $\Delta m=\pm 1$ induced by $\mathcal{H}_{1D}$. For example, the dashed line levels numbered 1 and 2 in the panel (a) are SO-coupled states with $m=-1|\downarrow\rangle$ and $m=0|\uparrow\rangle$, while the solid line levels 3 and 4 are SO-coupled states with $m=1|\downarrow\rangle$ and $m=2|\uparrow\rangle$, etc. In panel (b), the coupling conditions for dashed and solid lines are just exchanged with respect to spin orientation. Thus, for each energy level in subspace I, there is a degenerated mirror energy level in subspace II with spin orientation reversed. This double degeneracy is an inherent symmetry property due to the form of the Hamiltonian $\mathcal{H}_{1D}$ that replaces the pure doubly spin-degenerated states of $\mathcal{H}_0$. Thus, it is only necessary to calculate the energy spectrum for one of the Hilbert subspaces. In Fig. 2, we are showing how a change in the spatial confinement affects the spin splitting and the ordering of energy states caused by BIA term on the spectrum of a QR. It can be seen, from Figs. 1 and 2, that the interchange between levels (2,0) and $(1,\pm 4)$ as the aspect ratio r_2/r_1 is reduced. Also, the ordering of increasing energy levels can be modified not only by the ratio r_2/r_1 but also by the particular value of normalized BIA interaction parameter γ_D. Figure 3 is devoted to the energy splitting ΔE for the z component of the angular momentum $m=1$ and four quantum radial numbers $n=1,2,3,4$ as function of γ_D. Here, the stronger influence on ΔE corresponds to the excited states. Due to the competition between the states with different spin orientations provoked by $\mathcal{H}_{1D}$, the spin splitting must present a maximum at certain particular value of γ_D, which depends on the particular level under consideration. Comparing panels (a) and (b) in Fig. 3, the effect of the confinement on the energy spin splitting is clearly seen. Stronger confinement leads to larger energy spin-splitting. In our case, if we reduce the aspect ratio r_2/r_1 to a factor of 1.75, we obtain $\Delta E\sim 3$ times larger. Also, the maxima is right-hand shifted as the confinement increases, or r_2/r_1 decreases. As it is expected for large nonphysical value of the interaction parameter, the split energy ΔE tends to zero and the state remains with well defined spin orientation. Finally, let us point out that for large values of γ_D, the k-cubic term $\mathcal{H}_{3D}$ becomes important and must be included in the total Hamiltonian. In this sense, Figs. 1–3 have to be considered with caution. Moreover, very recently,

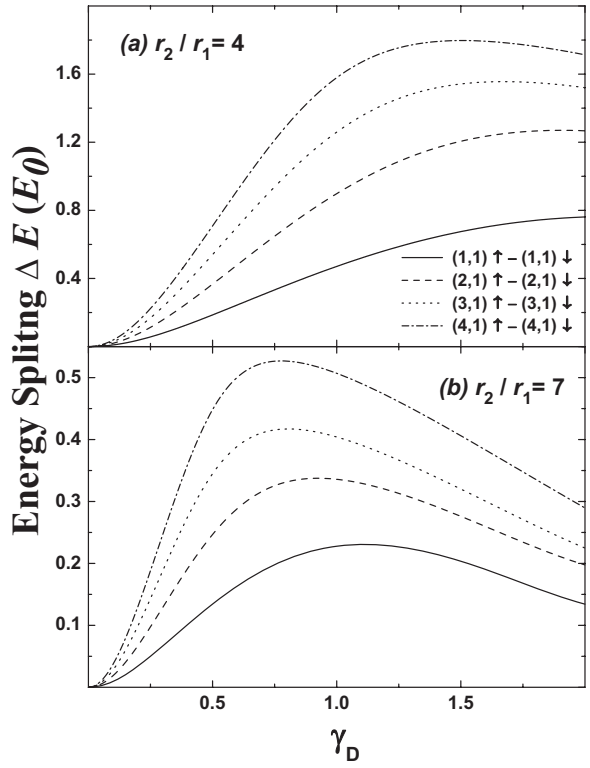

FIG. 3. Energy splitting in units of E_0 as a function of the dimensionless Dresselhaus parameter $\gamma_D = -\gamma/(r_1 E_0)$. The states $(n,m=1)$ with $n=1$, 2, 3, and 4 are considered. (a) QR aspect ratio $r_2/r_1=4$. (b) $r_2/r_1=7$.

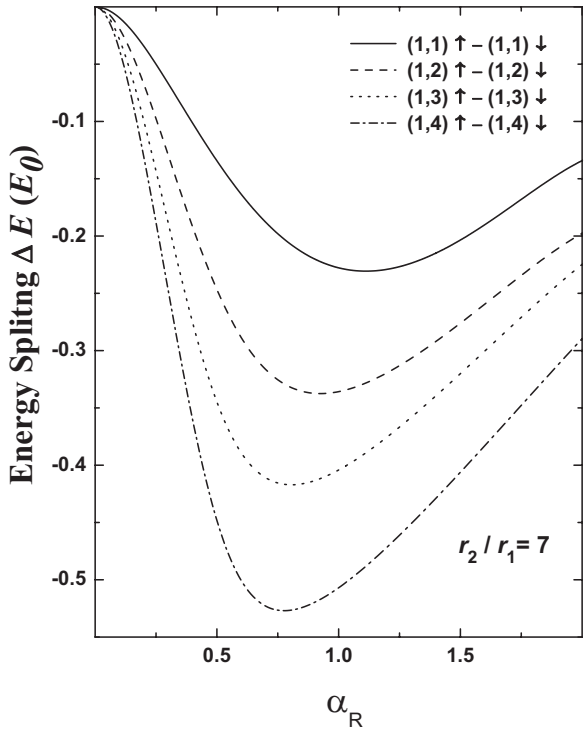

FIG. 4. Energy spin splitting due to Rashba interaction as a function of the dimensionless parameter $\alpha_R = \alpha e F / E_0$. The same states as in Fig. 3 are considered for a QR aspect ratio $r_2/r_1=7$.

the authors of Refs. 24 and 25 have stressed the effect of the k-cubic Dresselhaus term in GaAs/AlGaAs structures and have reported a value for the BIA parameter for GaAs three times smaller than the commonly used value of 27 eV Å.[3]

III. SPIN SPLITTING DUE TO THE RASHBA INTERACTION

There is another contribution that leads to the SO splitting which is provoked by the spatial asymmetry of the confinement potential **V** (space gradient) in semiconductor nanostructures and is called structural inversion asymmetry (SIA) or also referred as Rashba interaction.[7] This SO Hamiltonian is linear in the **k** wave vector as $\mathcal{H}_R = \alpha \mathbf{k} \times \nabla \mathbf{V} \cdot \sigma$, where α is the Rashba coupling parameter for the material. The inversion asymmetry potential can be characterized by certain effective electric field **F**, and for samples grown on the [001] crystal direction, we have $\mathbf{V}(\mathbf{z}) = V_o - eFz + \cdots$, where e is the bare electron charge. To lower order in **k** and F, the SIA spin-splitting Hamiltonian for QRs has the in-plane form

$$\mathcal{H}_R = -i\alpha e F(\hat{k}_+ \sigma_- - \hat{k}_- \sigma_+). \tag{14}$$

The SIA term can be modified not only by external electrical potentials[4,28,29] but also by modulation doping[27,29] or by the composition of heterostructure alloys.[30] The Hamiltonian (14) preserves the cylindrical symmetry as well as the time reversal property. Since the operator $\mathcal{H}_R$ has exactly the same mathematical structure as $\mathcal{H}_{1D}$ in Eq. (4), the eigenstates for $\mathcal{H} = \mathcal{H}_0 + \mathcal{H}_R$ have the form of Eq. (12); thus, the solutions may be constructed with a similar system of coupled equations (13), where a proper SIA normalized constant $\alpha_R = \alpha e F / E_0$ replaces the BIA constant $\gamma_D = -\gamma/(r_1 E_0)$ and with the interchange $f^- \Leftrightarrow f^+$. As shown in the Appendix, these matrix elements have the symmetry $f^+(m) = -f^-(-m)$; therefore, a state with given angular quantum number $|n,m,\downarrow\rangle$ is SO coupled to the state $|n,m+1,\uparrow\rangle$ by $\mathcal{H}_{1D}$ and is SO coupled to the state with $|n,m-1,\uparrow\rangle$ by $\mathcal{H}_R$. In this sense, the set of solutions is the same as the one presented in the previous section, but keeping the correct symmetric imposed by the SIA term. In order to visualize these properties, we present, in Fig. 4, the energy spin-splitting ΔE obtained with $\mathcal{H}_0 + \mathcal{H}_R$ as a function of the dimensionless Rashba parameter α_R for the same set of levels shown in Fig. 3. A quick comparison between Figs. 3(b) and 4 shows that both ΔE values have the same shape, tendency, and absolute values. For identical SO-coupling values and aspect ratio r_2/r_1, the spin-splitting ΔE induced by the Dresselhaus term is positive while by the Rashba term it is negative.

IV. COMPETITION BETWEEN BULK INVERSION ASYMMETRY AND STRUCTURAL INVERSION ASYMMETRY SPIN-ORBIT INTERACTIONS

When both Hamiltonians, $\mathcal{H}_R$ and $\mathcal{H}_D$, are added to the spin-degenerate Hamiltonian $\mathcal{H}_0$, it becomes clear that the quantum number m and the pure spin-up and spin-down components are mixed. In this axial broken symmetry, m and spin are no longer good quantum numbers. Nevertheless,

partial symmetry is preserved and the general form of the spinor Ψ is still grouped into two orthogonal Hilbert subspaces I and II and we can write

$$|\Psi_{\mathrm{I(II)}}\rangle = \sum_{n'} \sum_{m'=-\infty}^{\infty} \begin{bmatrix} a^{(1)}_{n',2m'(2m'+1)} |n', 2m'(2m'+1), \uparrow\rangle \\ a^{(2)}_{n',2m'+1(2m')} |n', 2m'+1(2m'), \downarrow\rangle \end{bmatrix}, \tag{15}$$

where the two subspaces I and II were defined following the parity of the quantum number m. States with even quantum number m and spin up are now SO coupled with all states with odd number m and spin-down, and vice versa. According to the wave function (15), the total Hamiltonian $\mathcal{H}_0+\mathcal{H}_R+\mathcal{H}_{1\mathrm{D}}$ provides for the new coefficients $a^{(i)}_{n',m'}(i=1,2)$ the following coupled system of equations:

$$(\mu_n^{(m)})^2 a^{(1)}_{n,m} + \sum_{n'} (i\gamma_D f^- a^{(2)}_{n',m+1} + \alpha_R f^+ a^{(2)}_{n',m-1}) = \lambda a^{(1)}_{n,m},$$

$$\sum_{n'} (-i\gamma_D f^+ a^{(1)}_{n',m} + \alpha_R f^- a^{(1)}_{n',m+2}) + (\mu_n^{(m+1)})^2 a^{(2)}_{n,m+1} = \lambda a^{(2)}_{n,m+1}. \tag{16}$$

Since $\mathcal{H}_D$ and $\mathcal{H}_R$ terms couple simultaneously states with different spin orientations, this results into an effective coupling that can, in principle, be tuned by external parameters. Once all states are SO coupled in one of the Hilbert subspace, then the *anticrossing* regions will appear between adjacent energy levels. In principle, and for a given value of the BIA coupling γ_D, the Rashba mechanism may be tuned to switched off or minimize the net SO mechanism. This effect is a fundamental issue to obtain a long spin lifetime for spin-field-effect devices.[4] In Fig. 5, we display the joint effects of both SO terms on energy spin splitting of the states $|1,1;\uparrow\downarrow\rangle$ as a function of the normalized Rashba parameter α_R for different values of γ_D. It can be seen that, for certain values of α_R, the spin splitting reaches a minimum, a consequence of the competition between the two SO mechanisms. These particular values of α_R, where the spin splittings induced by Rashba and Dresselhaus linear terms cancel each other out, depend on the parameter γ_D, on the particular spin-split state under consideration, and on the geometric ratio of the QR, r_2/r_1. These factors can be combined to implement a desired SFET in a two-dimensional systems where the conduction electrons will carry long spin lifetime.

Current efforts are in place in order to create a layered system based on a resonant tunneling diode with a layer of epitaxially grown nanoscopic QRs in the central well. This will allow the possibility of tuning the vertical transport properties through the system with the electronic levels in the rings. In this case, the gate voltage and the effective electric field created by charges built into the system will allow a tuning of the Rashba interaction. Built-in electric fields can be very strong in small regions of the tunneling diode; thus, the annihilation of the SO splitting can be attained as indicated in this work. This would lead to the control of the degeneracy of levels in the ring layer and, thus, of the density of transported charges. Nevertheless, the reliability of the proposed SFET devices depends on production of high mobility QRs.

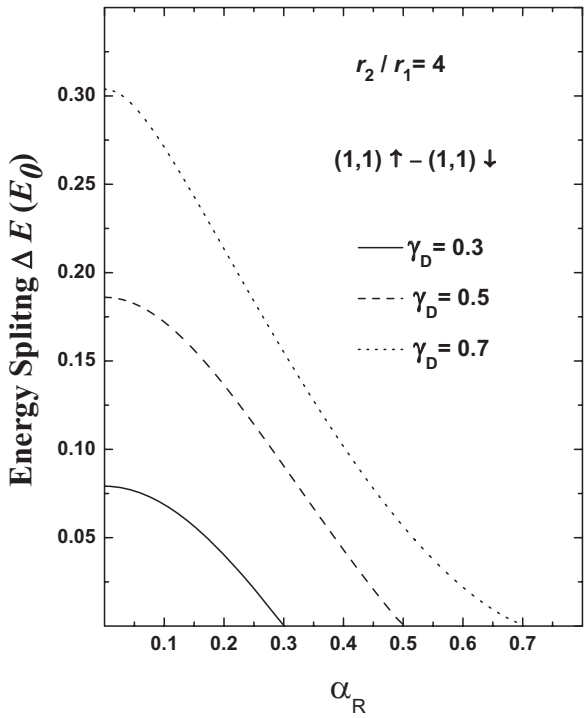

FIG. 5. Energy spin-splitting $\Delta E/E_0$ due to both effects Rashba and Dresselhaus interactions. $\Delta E/E_0$ is given as a function of $\alpha_R=\alpha eF/E_0$ for several values of the dimensionless parameter $\gamma_D=-\gamma/(r_1E_0)$. The states $|n,m=1;\uparrow\rangle$ and $|n=1,m=1;\downarrow\rangle$ were considered for a QR aspect ratio $r_2/r_1=4$.

The relative strengths of SO coefficients can be measured using, for example, the spin-galvanic and the circular photogalvanic effects induced by terahertz radiation.[26] Moreover, by detecting spin photocurrents, it is possible to infer under which circumstances the condition for equal contribution of Rashba and Dresselhaus interactions or for zero Rashba coefficient can be fulfilled.[27] It is important to remark that the problem of spin-resolved currents in a system where quantum mechanics governs the two dimensional motion of the electrons should be given careful attention in the future. It is known that QRs with three attached leads, one input and two outputs, can deliver spin-polarized beams of electrons.[11] In principle, and under the particular condition of zero SO interaction, a spin-polarized input state could be transmitted through the ring without substantial modification.

V. CONCLUSIONS

We have studied the influences of SIA and BIA SO interactions on the electronic spectrum of QRs with circular cross section. The electronic eigenenergies are determined by SO interactions, by the QR spatial confinement, and by the geometry factor r_2/r_1. The influence of the SO interactions (SIA and BIA) on the eigenenergies is enhanced as the aspect ratio r_2/r_1 is reduced and the system becomes more con-

fined. The absolute values of the energy splitting show a maximum for a particular value of the Rashba or Dresselhaus coefficients and their positions are shifted to lower values as r_2/r_1 increases. In the linear SO approximation for the electron momentum, the combined effects of SIA and BIA can lead to the complete annihilation of the energy spin splitting if the Rashba parameter α_R is properly tuned. The particular value of α_R where the energy spin splitting is zero depends on γ_D and on geometric ratio r_2/r_1. As we have noted, the parameter γ_D is proportional $\langle \hat{k}_z^2 \rangle = \langle \pi/L_z^2 \rangle$ and the position of the zero splitting can be tuned by the QR width. By increasing L_z (or smaller γ_D values), the position of α_R, where the zero spin splitting is observed in Fig. 5, moves toward smaller values. If a gate voltage (electric field) is applied perpendicular the QR plane and tuning the Rashba coefficient to equal the strength of Dresselhaus term, the parameter $\gamma = -\langle \hat{k}_z^2 \rangle \delta$ will also be affected by the field. In this case, a renormalization of the effective QR width takes place and L_z in $\langle \hat{k}_z^2 \rangle = \langle \pi/L_z^2 \rangle$ must be replaced by a shorter effective length $\tilde{L}_z$ given by[28]

$$\tilde{L}_z = L_z[1 + (0.12eFL_z/E_1^{(0)})^2]^{1/2}. \tag{17}$$

Finally, SFET devices based on QR structure can operate with an external gate voltage. Also by doping samples, and by changing the geometric factor r_2/r_1 or QR width L_z, both SO coefficients, α_R and γ_D, can be effectively tuned. Under the condition of mutually annihilating Rashba and linear Dresselhaus contributions, the neglected cubic term of Eq. (5) will restrict the long spin lifetime. The contribution of this cubic term, $\mathcal{H}_{3D}$, introduces an additional anisotropy to the ideal zero spin splitting here considered in Fig. 5. Thus, the inclusion of this Hamiltonian deserves further studies.

Another way to control the properties related to spin hybridization is by studying the effects of a magnetic field applied to the QR. This applied external potential should lift the partial degeneracy of states of the QR with circular cross section. The field will break the Kramers degeneracy and fully split the states into sets of spin up and spin down. Here, two limit situations can be considered: the field parallel or perpendicular to the QR growth direction. The magnetic field on the plane of the ring will modify the confined state along the z axis with energy $E_\nu^{(0)}$. Typical semiconductor QRs operate under the strong spatial confinement regime, i.e., the height $L_z \sim 0.5$ nm. In this case, the magnetic field represents a perturbation to the spatial confinement potential and a small shift to the energy $E_\nu^{(0)}$ is achieved. More interesting physical pictures are obtained when the external magnetic field is applied perpendicular to the growth direction. If the magnetic length l_e is larger than the outer radius r_2, $l_e \gg r_2$, we are within the weak field regime and the spatial confined potential prevails. Hence, the effects of the external potential on the energy levels can be handled by perturbation theory. The other limit corresponds to the ultrastrong magnetic field where $l_e \ll r_1$. Here, the width, $r_2 - r_1$, of the ring is negligible and the common theoretical treatment of the mesoscopic system for $r < r_1$ is recovered.[31] In the intermediate case where $r_2 < l_e < r_1$, the wave functions (7) do not represent a good basis and the full quantum mechanic calculation for the Schrödinger equation becomes necessary. The interplay between the spatial and magnetic confinements induces the energy levels to exhibit a complex dispersion as a function of the geometrical ring parameters and field intensity.

ACKNOWLEDGMENTS

The authors acknowledge financial support from Brazilian agencies FAPESP and CNPq. G.E.M. and C.T-G. are grateful to the Visiting Scholar Program of the ICTP/Trieste.

APPENDIX: MATRIX ELEMENTS

The matrix elements can be written as

$$\langle m', n' | k_x \pm k_y | n, m \rangle = -\frac{i}{r_1} \delta_{m', m \pm 1} f^{\mp}, \tag{A1}$$

with

$$f^{\mp} = \mp \int_{r1}^{r2} R_{n',m'} \left(\frac{\partial R_{n,m}}{\partial r} \mp \frac{m}{r} R_{n,m} \right) r dr. \tag{A2}$$

Using the general recurrence relations for the cylindrical functions[32]

$$\mathcal{Z}_{m+1}(z) + \mathcal{Z}_{m-1}(z) = \frac{2m}{z} \mathcal{Z}_m(z),$$

$$\mathcal{Z}_{m+1}(z) - \mathcal{Z}_{m-1}(z) = -2\frac{d\mathcal{Z}_m(z)}{dz}, \tag{A3}$$

we get that

$$f^{\mp} = \mp r_1^2 \mu_n^{|m' \mp 1|} A_{n',m'} A_{n,m' \mp 1} \times \int_1^{r_2/r_1} y \mathcal{Z}_{m'}(\mu_{n'}^{|m'|} y) \mathcal{Z}_{m'}(\mu_n^{|m' \mp 1|} y) dy. \tag{A4}$$

From[33]

$$\int y \mathcal{Z}_p(\alpha y) \mathcal{Z}_p(\beta y) dy = \frac{\beta y \mathcal{Z}_p(\alpha y) \mathcal{Z}_{p-1}(\beta y) + \alpha y \mathcal{Z}_{p-1}(\alpha y) \mathcal{Z}_p(\beta y)}{\alpha^2 - \beta^2}, \tag{A5}$$

we obtain that the matrix elements $f^{\mp}$ present the following closed analytical representation:

$$f^{\mp} = \mp \frac{r_1^2 \mu_{n'}^{|m'|} \mu_n^{|m'\mp 1|} A_{n',m'} A_{n,m'\mp 1}}{(\mu_{n'}^{|m'|})^2 - (\mu_n^{|m'\mp 1|})^2} \times \left[\frac{r_2}{r_1} C_{m'}\left(\mu_{n'}^{|m'|}, \frac{r_2}{r_1}\right) D_{m'}^{\mp}\left(\mu_n^{|m'\mp 1|}, \frac{r_2}{r_1}\right) - C_{m'}(\mu_{n'}^{|m'|}, 1) D_{m'}^{\mp}(\mu_n^{|m'\mp 1|}, 1) \right], \quad \text{(A6)}$$

where

$$D_m^{\mp}(\beta, t) = N_{|m\mp 1|}(\beta) J_{|m|}(\beta t) - J_{|m\mp|}(\beta) N_{|m|}(\beta t). \quad \text{(A7)}$$

From the above equations, we have the few useful symmetry properties

$$D_0^+ = D_0^-, \quad D_{-m}^+ = D_m^-, \quad C_{-m} = C_m, \quad \text{(A8)}$$

and

$$f^+(m) = -f^-(-m). \quad \text{(A9)}$$

[1] I. Žutić, J. Fabian, and S. Das Sarma, Rev. Mod. Phys. **76**, 323 (2004).
[2] V. A. Guzenko, J. Knobbe, H. Hardtdegen, Th. Schäpers, and A. Bringer, Appl. Phys. Lett. **88**, 032102 (2006).
[3] X. W. Zhang, S. S. Li, and J. B. Xia, Appl. Phys. Lett. **89**, 172113 (2006).
[4] J. Schliemann, J. C. Egues, and D. Loss, Phys. Rev. Lett. **90**, 146801 (2003).
[5] C. F. Destefani, S. E. Ulloa, and G. E. Marques, Phys. Rev. B **69**, 125302 (2004).
[6] R. de Sousa and S. Das Sarma, Phys. Rev. B **68**, 155330 (2003).
[7] Yu. A. Bychkov, and E. I. Rashba, Sov. Phys. JETP **39**, 78 (1984); J. Phys. C **17**, 6039 (1984).
[8] G. Dresselhaus, Phys. Rev. **100**, 580 (1955).
[9] S. Datta and B. Das, Appl. Phys. Lett. **56**, 665 (1990).
[10] S. Ree and L. E. Reichl, Phys. Rev. B **59**, 8163 (1999).
[11] P. Földi, O. Kalman, M. G. Benedict, and F. M. Peeters, Phys. Rev. B **73**, 155325 (2006).
[12] M. Persson, J. Pettersson, B. von Sydow, P. E. Lindelof, A. Kristensen, and K. F. Berggren, Phys. Rev. B **52**, 8921 (1995); K. F. Berggren, Z. L. Ji, and T. Lundberg, *ibid.* **54**, 11612 (1996).
[13] J. M. García, G. Medeiros-Ribeiro, K. Schmidt, T. Ngo, J. L. Feng, A. Lorke, J. Kotthaus, and P. M. Petroff, Appl. Phys. Lett. **71**, 2014 (1997).
[14] A. Lorke and R. J. Luyken, Physica B **256-258**, 424 (1998); A. Lorke, R. J. Luyken, M. Fricke, J. P. Kotthaus, G. Medeiros-Ribeiro, J. M. García, and P. M. Petroff, Microelectron. Eng. **47**, 95 (1999).
[15] H. Pettersson, R. J. Warburton, A. Lorke, K. Karrai, J. P. Kotthaus, J. M. García, and P. M. Petroff, Physica E (Amsterdam) **6**, 510 (2000).
[16] A. Lorke, R. J. Luyken, A. O. Govorov, J. P. Kotthaus, J. M. García, and P. M. Petroff, Phys. Rev. Lett. **84**, 2223 (2000).
[17] R. J. Warburton, C. Schaflein, D. Haft, F. Bickel, A. Lorke, K. Karrai, J. M. García, W. Schoenfeld, and P. M. Petroff, Nature (London) **405**, 926 (2000).
[18] J. C. Ahn, K. S. Kwak, B. H. Park, H. Y. Kang, J. Y. Kim, and O. D. Kwon, Phys. Rev. Lett. **82**, 536 (1999).
[19] A. Lorke and R. J. Luyken, Physica B **256**, 424 (1998).
[20] P. Foldi, B. Molnár, M. G. Benedict, and F. M. Peeters, Phys. Rev. B **71**, 033309 (2005).
[21] J. M. Llorens, C. Trallero-Giner, A. García-Cristóbal, and A. Cantarero, Phys. Rev. B **64**, 035309 (2001).
[22] E. Menéndez-Proupin, C. Trallero-Giner, and S. E. Ulloa, Phys. Rev. B **60**, 16747 (1999).
[23] Note the missing $1/r_1$ factor in the normalization constant reported in Ref. 21.
[24] D. M. Zumbühl, J. B. Miller, C. M. Marcuset, D. Goldhaber-Gordon, J. S. Harris, Jr., K. Campman, and A. C. Gossard, Phys. Rev. B **72**, 081305(R) (2005).
[25] J. J. Krich and B. I. Halperin, Phys. Rev. Lett. **98**, 226802 (2007).
[26] S. D. Ganichev, V. V. Bel'kov, L. E. Golub, E. L. Ivchenko, P. Schneider, S. Giglberger, J. Eroms, J. De Boeck, G. Borghs, W. Wegscheider, D. Weiss, and W. Prettl, Phys. Rev. Lett. **92**, 256601 (2004); S. D. Ganichev, E. L. Ivchenko, V. V. Bel'kov, S. A. Tarasenko, M. Sollinger, D. Weiss, W. Wegscheider, and W. Prettl, Nature (London) **417**, 153 (2002).
[27] S. Giglberger, L. E. Golub, V. V. Bel'kov, S. N. Danilov, D. Schuh, C. Gerl, F. Rohlfing, J. Stahl, W. Wegscheider, D. Weiss, W. Prettl, and S. D. Ganichev, Phys. Rev. B **75**, 035327 (2007).
[28] F. M. Alves, G. E. Marques, V. López-Richard, and C. Trallero-Giner, Semicond. Sci. Technol. **22**, 301 (2007).
[29] H. B. de Carvalho, M. J. S. P. Brasil, V. Lopez-Richard, Y. Galvão Gobato, G. E. Marques, I. Camps, L. C. O. Dacal, M. Henini, L. Eaves, and G. Hill, Phys. Rev. B **74**, 041305(R) (2006).
[30] H. H. Nilsson, J. Z. Zhang, and I. Galbraith, Phys. Rev. B **72**, 205331 (2005).
[31] J. S. Sheng and K. Chang, Phys. Rev. B **74**, 235315 (2006).
[32] M. Abramowitz and I. Stegun, *Handbook of Mathematical Functions* (Dover, New York, 1972).
[33] I. S. Gradshteyn and I. M. Ryzhik, *Tables of Integrals, Series and Products* (Academic, New York, 1980).